

Infrared lattice vibrations and dielectric dispersion in α -Fe₂O₃

Seinosuke Onari, Toshihiro Arai, and Keiei Kudo

Institute for Optical Research, Kyoiku University, 3-22-17 Shinzyuku-ku, Tokyo
and Institute of Applied Physics, the University of Tsukuba, Academic Town, Ibaragi, Japan

(Received 15 March 1977)

The infrared reflection spectra of α -Fe₂O₃ were measured in the energy range 30–1000 cm⁻¹; two optical-phonon modes were observed for extraordinary ray; four optical-phonon modes were observed for ordinary ray. The optical constants were calculated by Kramers-Kronig analysis, and were also analyzed by the classical-oscillator model. From these dielectric constants, the longitudinal and transverse optical-phonon frequencies were estimated. The Born and Szigeti effective charges were calculated and the ionicities among α -Fe₂O₃, α -Cr₂O₃, and α -Al₂O₃ were studied. It is verified also that the generalized Lyddane-Sachs-Teller equation apply very well to α -Fe₂O₃.

I. INTRODUCTION

Crystals of α -Fe₂O₃, α -Cr₂O₃, and α -Al₂O₃ have the corundum¹ structure and crystallize into the trigonal system with the space group D_{3d}^6 . A unit cell contains ten atoms.

The infrared lattice vibration spectra of α -Al₂O₃,^{2,3} and α -Cr₂O₃,⁴ have been studied well by several workers. The reflectivity of α -Fe₂O₃ has been reported by Mitsuishi *et al.*³ in the wavelength range from 17 to 50 μ m, which however did not cover the whole lattice vibration frequency. Also, they did not determine the optical constants. Recently the optical constants of α -Fe₂O₃ were reported by Popova *et al.*,⁵ however, their data disagree with those by Mitsuishi *et al.* in many points. We can notice the absence of 43- μ m structure in Popova's data and the significant difference in the region from 20 to 30 μ m. There is also a confusion in Popova's paper concerning the definition of ordinary and extraordinary ray.

In the present work it was undertaken to discover all the normally allowed infrared vibration modes of the α -Fe₂O₃ and to determine the optical constants throughout the region of the lattice vibrations. The factor group analysis of the normal modes of corundum was made by Bhagavantam and Venkatarayuku.⁶ A decomposition into irreducible representations gives

$$\Gamma = 2A_{1g} + 2A_{1u} + 3A_{2g} + 3A_{2u} + 5E_g + 5E_u,$$

and there are 18 distinct normal frequencies at the Γ point. A one-dimensional A_{2u} and a two-dimensional E_u mode correspond to the acoustic phonons. Two one-dimensional A_{1g} and five two-dimensional E_g modes are Raman active. Two one-dimensional A_{2u} and four two-dimensional E_u modes are infrared active.

α -Fe₂O₃ and α -Cr₂O₃ are high-resistivity magnetic semiconductors⁷ with electric conductivity similar to that of Cu₂O. The magnetic properties

of these materials have been studied extensively. Below the Morin⁸ transition (260 K) the four iron atoms, spin $\frac{5}{2}$, align along the C axis in a (+ - - +) antiferromagnetic arrangement.⁹ Between 260 K and the Néel temperature (950 K) the spins lie in the basal plane with a slight canting which results in a small ferromagnetic moment.¹⁰

Two magnon and first-order phonon Raman scattering in α -Fe₂O₃ have been reported by Hart *et al.*¹¹ and are compared to the theoretical predictions. Polarization studies show that the two A_{1g} phonon modes lie at 225 and 498 cm⁻¹, and the five E_g phonon modes lie at 247, 293, 299, 412, and 613 cm⁻¹.

In this work four E_u phonons and two A_{2u} phonons were observed in the reflection spectrum with the electric vector E of the incident light perpendicular and parallel to the C axis, respectively. This is consistent with the group-theoretical prediction on the allowed infrared modes.

A Kramers-Kronig analysis and a classical-oscillator fit were performed to obtain the optical constants of α -Fe₂O₃. The Born and Szigeti effective charges were calculated for α -Fe₂O₃, α -Cr₂O₃, and α -Al₂O₃ to study the ionicity, and the Born effective charge of α -Al₂O₃ agrees well with the charge parameter obtained in the calculation of the lattice dynamics.¹² It is also shown that the generalized Lyddane-Sachs-Teller relation applies very well to the spectra of α -Fe₂O₃.

II. EXPERIMENTS

The measurement of the infrared reflection spectra at room temperature was performed with a Digilab Fourier-transform spectrometer FTS 16B in the energy range from 1000 to 30 cm⁻¹. An aluminum mirror was used as a reference in the reflection measurement. A transmission wire grating polarizer with 720 lines per mm and polarization efficiency better than 95% was used to

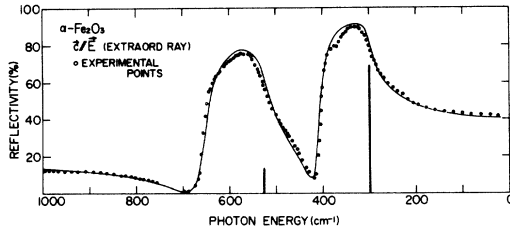


FIG. 1. Reflection spectrum of α - Fe_2O_3 for the extraordinary ray with the electric vector E of the incident light parallel to the C axis. The solid curve is the reflection calculated by the classical-oscillator model. The vertical bars indicate the transverse-optical-phonon frequencies and strength.

select the reflectivity for the electric vector E of the incident light perpendicular and parallel to the crystallographic C axis.

The samples used were good-quality natural hematite from the National Science Museum in Tokyo. The good natural surface is at an angle (approximately 16°) with respect to the surface perpendicular to the C axis. We can see a pattern of many straight lines on this surface and they lie on the plane perpendicular to the C axis. From this pattern on the two different planes and in the different directions of a single crystal, we can easily determine the surface perpendicular to the C axis. This simple way of crystal axis determination was also confirmed by x-ray Laue-pattern measurement, and both results were in good agreement. As no extra lines of the impurities could be observed in the x-ray powder Debye-Scherrer spectrum, the concentration of the impurities is considered very small. No difference is reported² between the spectra of ruby and those of pure α - Al_2O_3 till the impurity concentration of 1.3%, therefore the impurity effect on the spectra of α - Fe_2O_3 may also be negligible.

III. RESULTS AND DISCUSSIONS

As the crystal lattice of α - Fe_2O_3 belongs to the trigonal system,¹ any macroscopic second-rank tensor properties such as the dielectric constant (ϵ) will have two independent parts. Two independent measurements of ϵ , one with the electric vector E along the crystalline C axis and the other with the electric vector E in any direction in the plane perpendicular to the C axis, will completely specify the dielectric tensor.

The most elementary approach to the optical properties of ionic crystals is to consider a single classical oscillator and solve the equation of motion to obtain the Lorentz formula for the real (ϵ_1) and imaginary parts (ϵ_2) of the dielectric constant. A series of classical oscillators are

needed for the complex crystals of the trigonal system to explain the observed optical dispersion, and this is expressed by the following formula:

$$\epsilon_1 + i\epsilon_2 = \epsilon_\infty + \sum_{\nu=1} \frac{4\pi\rho_\nu\omega_{T\nu}^2}{(\omega_{T\nu}^2 - \omega^2) - i\gamma_\nu\omega}, \quad (1)$$

where $\omega_{T\nu}$ is the transverse optical-phonon frequency corresponding to the peak of ϵ_2 . $4\pi\rho_\nu$ and γ_ν are the strength and linewidth, respectively, of the ν th oscillator, and ϵ_∞ is the high-frequency dielectric constant. Subscripts \parallel and \perp should be applied to all the quantities in Eq. (1) except ω for the $\vec{E} \parallel \vec{C}$ and $\vec{E} \perp \vec{C}$ configurations, respectively.

From the well-known relations

$$\epsilon_1 + i\epsilon_2 = (n + ik)^2$$

and

$$R = [(n-1)^2 + k^2] / [(n+1)^2 + k^2],$$

we can calculate the power reflectivity R at normal incidence.

In Fig. 1 the reflection spectrum of α - Fe_2O_3 for electric vector E of the incident light parallel to the C axis is shown. From this reflection spectrum the optical constants were first determined by a Kramers-Kronig analysis,¹³ and then the classical-oscillator fit was performed as follows to obtain better optical constants. For initial values of the parameters in Eq. (1) we used the dielectric constants from the Kramers-Kronig analysis, and better parameters which improve the fit to the reflection spectrum were looked for until the fit became satisfactory.

A similar analysis was performed of the reflection spectrum of α - Fe_2O_3 for electric vector E of the incident light perpendicular to the C axis, and this is shown in Fig. 2. The solid line is the reflectivity calculated from the classical-oscillator model, and the circles are the experimental reflectivity. The classical-oscillator parameters obtained here for α - Fe_2O_3 are listed in Table I

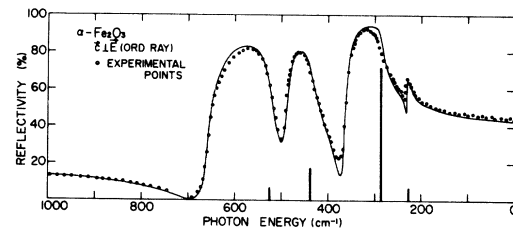


FIG. 2. Reflection spectrum of α - Fe_2O_3 for the ordinary ray with the electric vector E of the incident light perpendicular to the C axis. The solid curve is the reflection calculated by the classical-oscillator model. The vertical bars indicate the transverse-optical-phonon frequencies and strength.

TABLE I. Parameters of the classical oscillators in Eq. (1) for α -Al₂O₃ by Barker (Ref. 2), α -Cr₂O₃ by Renneke (Ref. 4), and α -Fe₂O₃. $\omega(\text{LO})$ is the longitudinal-optical frequency determined from the peak frequency of $\text{Im}(-1/\epsilon)$. ϵ_0 is the dielectric constant in the low-frequency region and has the relation

$$\epsilon_0 = \epsilon_\infty + \sum_{\nu} 4\pi p_{\nu}.$$

α -Al ₂ O ₃		α -Cr ₂ O ₃		α -Fe ₂ O ₃	
$\omega_{\nu}(\text{TO})$ (cm ⁻¹)	$\omega_{\nu}(\text{LO})$ (cm ⁻¹)	$\omega_{\nu}(\text{TO})$ (cm ⁻¹)	$\omega_{\nu}(\text{LO})$ (cm ⁻¹)	$\omega_{\nu}(\text{TO})$ (cm ⁻¹)	$\omega_{\nu}(\text{LO})$ (cm ⁻¹)
ϵ_∞	ϵ_0	ϵ_∞	ϵ_0	ϵ_∞	ϵ_0
γ (cm ⁻¹)	$4\pi p_{\nu}$	γ (cm ⁻¹)	$4\pi p_{\nu}$	γ (cm ⁻¹)	$4\pi p_{\nu}$
400	512	538	602	299	414
583	871	613	759	526	662
3.1	11.6	6.1	11.7	6.7	20.6
8.0	20.4	18		15	
20.4		9		30	
0.3	0.3	0.4	0.4	1.1	1.1
2.7	2.7	0.15	0.15	12.0	12.0
3.0	3.0	5.45	5.45	2.9	2.9
11.4	11.4	0.5	0.5	1.1	1.1
12.7	12.7	6.2	12.7	7.0	24.1

($\vec{E} \parallel \vec{C}$)

($\vec{E} \perp \vec{C}$)

together with the values for α -Al₂O₃ by Barker² and α -Cr₂O₃ by Renneke⁴ for comparison. The high-frequency dielectric constant ϵ_∞ of α -Al₂O₃ is about two times smaller than those of α -Cr₂O₃ and α -Fe₂O₃. The low-frequency dielectric constants ϵ_0 of α -Al₂O₃ and α -Cr₂O₃ are nearly the same but that of α -Fe₂O₃ is approximately two times larger.

In the system of n atoms (ions) in a unit cell, the polarization is given by

$$P = (1/4\pi)(\epsilon_\infty - 1)E + N \sum_i e_i^* x_i \quad (2)$$

and the dielectric function is given by Eq. (1), with the substitution

$$4\pi p_{\nu} \omega_{\nu}^2 = \left(\sum_i e_i^* x_{i\nu} \right)^2 \left(\sum_i M_i x_{i\nu}^2 \right)^{-1},$$

where e_i^* and M_i correspond to the charge and mass of the i th ion and $x_{i\nu}$ corresponds to the displacement of the i th ion in the ν th vibration.

The longitudinal-optical-phonon frequency ω_L is obtained by the following relation for the case of no damping:

$$\frac{4\pi N}{\epsilon_\infty} \sum_{\nu} \frac{\left(\sum_i e_i^* x_{i\nu} \right)^2}{\left(\sum_i M_i x_{i\nu}^2 \right)^{-1}} \frac{1}{(\omega_{\nu}^2 - \omega_L^2)} = 1. \quad (3)$$

This condition also satisfies the criterion for the longitudinal-optical phonon $\epsilon(\omega_L) = 0$. For oscillators with a small damping, almost the same LO frequencies are obtained from the maximum of $\text{Im}(-1/\epsilon)$.

With these longitudinal-optical-phonon frequencies and the transverse-optical-phonon frequencies derived from Eq. (1), the relevant relation between the effective charges of the ions and the optical data can be expressed as follows¹⁴:

$$4\pi N \sum_i \frac{e_i^{*2}}{M_i} = \epsilon_\infty \sum_{\nu} (\omega_{L\nu}^2 - \omega_{T\nu}^2), \quad (4)$$

where N is the number of unit cells in a unit volume, M_i is the mass of the i th ion, and the summation is over all the ions in a unit cell. It is easily verified for the case of one infrared mode and one ion pair that this formula reduces to the well-known equation for the Born effective charge¹⁵ e_B^* which corresponds to the effective charge of the transverse wave, and is directly related to the optical and dielectric properties of the crystal. When we apply this formula to α -Fe₂O₃, we can use the relation between charges determined from the neutrality condition $3e_O^* + 2e_{Fe}^* = 0$, where e_O^* and e_{Fe}^* are the effective charges of oxygen and iron.

From this neutrality condition, we can obtain the relation

$$32\pi Ne_{\text{Fe}}^{*2} \left(\frac{1}{3M_{\text{O}}} + \frac{1}{2M_{\text{Fe}}} \right) = \epsilon_{\infty} \sum_{\nu} (\omega_{L\nu}^2 - \omega_{T\nu}^2), \quad (5)$$

where M_{O} and M_{Fe} are the masses of the oxygen and iron ions. The factor in parentheses on the left-hand side of this equation corresponds to the inverse of the reduced mass of the two iron atoms and the three oxygen atoms. The calculated effective charges of the Fe ion are $e_{\text{Fe}}^* = 3.75e$ and $e_{\text{Fe}}^* = 4.05e$ for $\vec{E} \parallel \vec{C}$ and $\vec{E} \perp \vec{C}$, respectively, where e is the charge of an electron.

We also performed a similar calculation of the effective charge on $\alpha\text{-Cr}_2\text{O}_3$ and $\alpha\text{-Al}_2\text{O}_3$ and the results are listed in Table II. In all three materials the Born effective charge obtained from the $\vec{E} \perp \vec{C}$ spectrum is slightly larger than that obtained from the $\vec{E} \parallel \vec{C}$ spectrum, $\alpha\text{-Cr}_2\text{O}_3$ has more charge than $\alpha\text{-Al}_2\text{O}_3$, and $\alpha\text{-Fe}_2\text{O}_3$ has more charge than $\alpha\text{-Cr}_2\text{O}_3$.

The charge parameter calculated by Kappus¹² in lattice dynamics for $\alpha\text{-Al}_2\text{O}_3$ is $2.053e$. In the lattice-dynamics calculation the experimentally obtained dielectric constant ϵ_{∞} is not taken into account explicitly,¹⁶ therefore a correction to the charge for this shielding effect on the Coulomb interaction is necessary in order to compare this charge. The correction is to multiply $\sqrt{\epsilon_{\infty}}$ by the charge parameter and one obtains $3.65e$ for $\alpha\text{-Al}_2\text{O}_3$. This value is in good agreement with the Born effective charge of $3.35e$ and $3.37e$ calculated by the optical data.

To discuss the microscopic properties of the polarization, the Szigeti effective charge¹⁷ defined by the relation

$$e_s^* = [3/(\epsilon_{\infty} + 2)] e_B^* \quad (6)$$

is more appropriate. This charge is considered to have a precise meaning for cubic and typically ionic crystals. The physical meaning of this charge becomes a little ambiguous for uniaxial crystals. However it seems worthwhile to calculate this charge for the above three materials because the dielectric constant ϵ_{∞} and the effective charge e_B^* calculated in the two directions $\vec{E} \parallel \vec{C}$ and $\vec{E} \perp \vec{C}$ are almost the same, and almost isotro-

TABLE II. The Born and Szigeti effective charge for $\alpha\text{-Fe}_2\text{O}_3$, $\alpha\text{-Cr}_2\text{O}_3$, and $\alpha\text{-Al}_2\text{O}_3$ calculated from the data in Table I and Eqs. (5) and (6). e is the free-electron charge. \parallel and \perp correspond to orientation parallel and perpendicular to the C axis, respectively.

	$e_{B\parallel}^*/e$	$e_{B\perp}^*/e$	$e_{S\parallel}^*/e$	$e_{S\perp}^*/e$
$\alpha\text{-Fe}_2\text{O}_3$	3.75	4.05	1.29	1.35
$\alpha\text{-Cr}_2\text{O}_3$	3.65	3.82	1.35	1.40
$\alpha\text{-Al}_2\text{O}_3$	3.35	3.37	1.97	1.94

pic. The calculated value of the Szigeti effective charge are listed in Table II.

It is interesting to notice that the degree of the ionicity is in the inverse order among these three materials in the Szigeti effective charge and the Born transverse effective charge. This is due to the dielectric shielding effect. If these materials are completely ionic the Szigeti effective charge on the Fe^{3+} ion will become $3e$. The obtained smaller value of this charge means that the band nature of these materials is partly ionic and partly covalent.

Symmetry analysis¹⁸ verifies for the A_{2u} mode that Fe atoms vibrate in the direction of the C axis and the group of three oxygen atoms has the mixed motion in the direction of the C axis associated with the rotation motion around the C axis. No relative vibration between iron ions, and no relative vibration between oxygen atoms are predicted from symmetry considerations.

In the E_u mode the motion of the iron ions is in the plane perpendicular to the C axis, and the motion of the oxygen ions is a little complicated as in calcite.^{18,19} The vibration frequencies may be mainly influenced by the force constant between oxygen ions and iron ions.

The frequencies of $\alpha\text{-Fe}_2\text{O}_3$ are smaller than those of $\alpha\text{-Cr}_2\text{O}_3$ as shown in Table I. The difference in vibration frequencies between $\alpha\text{-Al}_2\text{O}_3$ and $\alpha\text{-Cr}_2\text{O}_3$ might be attributed to the difference in the weight of Al and Cr ions, and also to the difference in the interionic force constants. When we compare Cr_2O_3 and Fe_2O_3 the atomic weight of Cr and Fe is almost the same, and the difference in frequency should be related to the difference in force constants. The interionic distance between the oxygen and metal ion is 2.09, 2.01, and 1.97 Å for $\alpha\text{-Fe}_2\text{O}_3$, $\alpha\text{-Cr}_2\text{O}_3$, and $\alpha\text{-Al}_2\text{O}_3$, respectively.

It is known that the increase in interionic distance reduces the force constants between pairs of ions both for ionic bonding and covalent bonding.²⁰ The weaker force constant in $\alpha\text{-Fe}_2\text{O}_3$ may be attributed to the longer bond length between Fe and O ions.

In the case of $\alpha\text{-Al}_2\text{O}_3$ and $\alpha\text{-Cr}_2\text{O}_3$ forbidden modes were reported in the reflection spectrum,^{2,4} however no appreciable forbidden modes could be observed in $\alpha\text{-Fe}_2\text{O}_3$. The small structure in the $\vec{E} \parallel \vec{C}$ spectrum at 370 cm^{-1} may be due to a slight mixing of the sharp dip in the $\vec{E} \perp \vec{C}$ reflection spectrum.

When the damping of the oscillators is small, generalized Lyddane-Sachs-Teller relations^{14,21} for uniaxial crystals with many lattice vibration modes can be written as follows for each component $\vec{E} \parallel \vec{C}$ and $\vec{E} \perp \vec{C}$:

TABLE III. Comparison of the right- and left-hand sides of Eq. (7) for α -Fe₂O₃.

Orientation	$\frac{\epsilon_0}{\epsilon_\infty}$	$\prod_\nu \left(\frac{\omega_\nu(\text{LO})}{\omega_\nu(\text{TO})} \right)^2$
$\vec{E} \parallel \vec{C}$	3.07	3.04
$\vec{E} \perp \vec{C}$	3.44	3.45

$$\prod_\nu \left(\frac{\omega_\nu(\text{LO})}{\omega_\nu(\text{TO})} \right)^2 = \frac{\epsilon_0}{\epsilon_\infty}, \quad (7)$$

where the product is over all the infrared-active modes. The values of each side of this equation

for both configurations $\vec{E} \parallel \vec{C}$ and $\vec{E} \perp \vec{C}$ are shown in Table III. The correction by damping terms to the Lyddane-Sachs-Teller relations has been reported by Chang *et al.*,²² and the correction estimated in our case is of order 10^{-3} . The very small discrepancy of 0.03 between the right- and left-hand terms of Eq. (7) may be the experimental error, and the agreement is quite satisfactory.

ACKNOWLEDGMENT

We would like to express sincere thanks to Dr. S. Matsubara of the National Science Museum for supplying us the α -Fe₂O₃ crystals.

- ¹R. W. G. Wyckoff, *Crystal Structures* (Wiley, New York, 1963), Vol. 2, p. 7.
- ²A. S. Barker, Jr., *Phys. Rev.* **132**, 1474 (1963).
- ³A. Mitsuishi, H. Yoshinaga, S. Fujita, and Y. Suemoto, *Jpn. J. Appl. Phys.* **1**, 1 (1962).
- ⁴D. R. Renneke and D. W. Lynch, *Phys. Rev.* **138**, A530 (1965).
- ⁵S. I. Popova, T. S. Tolstykh, and L. S. Ivlev, *Opt. Spektrosk.* **35**, 551 (1973).
- ⁶S. Bhagavantam and T. Venkatarayuku, *Proc. Indian Acad. Sci. A* **9**, 224 (1939).
- ⁷D. Adler, in *Solid State Physics*, edited by F. Seitz *et al.* (Academic, New York, 1968), Vol. 21, p. 79; H. J. van Daal and A. J. Bosman, *Phys. Rev.* **158**, 736 (1967).
- ⁸F. J. Morin, *Phys. Rev.* **78**, 819 (1950).
- ⁹C. G. Shull, W. A. Strauser, and E. O. Wollan, *Phys. Rev.* **83**, 333 (1951).
- ¹⁰I. Dzialoshinski, *J. Phys. Chem. Solids* **4**, 241 (1958).
- ¹¹T. R. Hart, S. B. Adams, and H. Temkin, in *Light Scattering in Solids*, edited by M. Balkanski *et al.* (Flammarion, Paris, 1975), p. 259.
- ¹²H. Bialas and H. J. Stolz, *Z. Phys.* **B21**, 319 (1975); W. Kappus, *ibid.* **B21**, 325 (1975).
- ¹³S. Onari *et al.*, *J. Phys. Soc. Jpn.* **37**, 1585 (1974).
- ¹⁴T. Kurosawa, *J. Phys. Soc. Jpn.* **16**, 1298 (1961).
- ¹⁵M. Born and K. Huang, *Dynamical Theory of Crystal Lattices* (Oxford University, London, 1954).
- ¹⁶A. A. Maradudin *et al.*, in *Solid State Physics*, 2nd ed., edited by F. Seitz and D. Turnbull (Academic, New York, 1971), Suppl. 3.
- ¹⁷B. Szigei, *Trans. Faraday Soc.* **45**, 155 (1949); B. Szigei, *Proc. R. Soc. A* **204**, 51 (1950).
- ¹⁸E. R. Cowley, *Can. J. Phys.* **47**, 1381 (1969).
- ¹⁹M. Onomichi, *Sci. Light* **22**, 47 (1973).
- ²⁰L. Pauling, *Nature of the Chemical Bond*, 2nd ed. (Cornell University, Ithaca, 1948); W. Gordy, *J. Chem. Phys.* **14**, 305 (1946).
- ²¹R. H. Lyddane, R. G. Sachs, and E. Teller, *Phys. Rev.* **59**, 673 (1941); W. Cochran, *Z. Krist.* **112**, 465 (1959).
- ²²I. F. Chang *et al.*, *Phys. Status Solidi* **28**, 663 (1968).